

The supergiant B[e] star LHA 115-S 18 - binary and/or luminous blue variable?★

J. S. Clark¹, E. S. Bartlett², M. J. Coe², R. Dorda³, F. Haberl⁴, J. B. Lamb⁵, I. Negueruela³, and A. Udalski⁶

¹Department of Physics and Astronomy, The Open University, Walton Hall, Milton Keynes, MK7 6AA, United Kingdom

²The Faculty of Physical and Applied Sciences, University of Southampton, Highfield, Southampton, S017 1BJ, United Kingdom

³Departamento de Física, Ingeniería de Sistemas y Teoría de la Señal, Universidad de Alicante, Apdo. 99, E03080 Alicante, Spain

⁴Max-Planck-Institut für extraterrestrische Physik, Postfach 1312, Giessenbachstr., 85741 Garching, Germany

⁵Department of Astronomy, University of Michigan, 830 Dennison Building, Ann Arbor, MI 48109-1042, USA

⁶Warsaw University Observatory, Aleje Ujazdowskie 4, 00-478 Warsaw, Poland

Preprint online version: April 25, 2013

ABSTRACT

Context. The mechanism by which supergiant (sg)B[e] stars support cool, dense dusty discs/tori and their physical relationship with other evolved, massive stars such as luminous blue variables is uncertain.

Aims. In order to investigate both issues we have analysed the long term behaviour of the canonical sgB[e] star LHA 115-S 18.

Methods. We employed the OGLE II-IV lightcurve to search for (a-)periodic variability and supplemented these data with new and historic spectroscopy.

Results. In contrast to historical expectations for sgB[e] stars, S18 is both photometrically and spectroscopically highly variable. The lightcurve is characterised by rapid aperiodic ‘flaring’ throughout the 16 years of observations. Changes in the high excitation emission line component of the spectrum imply evolution in the stellar temperature - as expected for luminous blue variables - although somewhat surprisingly, spectroscopic and photometric variability appears not to be correlated. Characterised by emission in low excitation metallic species, the cool circumstellar torus appears largely unaffected by this behaviour. Finally, in conjunction with intense, highly variable He II emission, X-ray emission implies the presence of an unseen binary companion.

Conclusions. S18 provides observational support for the putative physical association of (a subset of) sgB[e] stars and luminous blue variables. Given the nature of the circumstellar environment of S18 and that luminous blue variables have been suggested as SN progenitors, it is tempting to draw a parallel to the progenitors of SN1987A and SN2009ip. Moreover the likely binary nature of S18 strengthens the possibility that the dusty discs/tori that characterise sgB[e] stars are the result of binary-driven mass-loss; consequently such stars may provide a window on the short lived phase of mass-transfer in massive compact binaries.

Key words. stars:evolution - stars:early type - stars:binary - star:individual:LHA 115-S 18 - star:emission-line

1. Introduction

Supergiant (sg)B[e] stars are thought to represent a short lived phase in the evolution of massive stars from the main sequence through to H-depleted Wolf-Rayets (WR). Observationally, they are characterised by an hybrid spectrum consisting of broad emission lines in high excitation species and narrow, low excitation metallic lines and a near-mid IR continuum excess. Zickgraf et al. (1985) proposed a two component circumstellar environment to reconcile these findings, comprising a hot, high velocity polar wind and a low velocity equatorial disc or torus. The latter is expected to be either slowly expanding or in quasi-Keplerian rotation (Zickgraf et al 2003, Kraus et al. 2010, Aret et al. 2012) and appears to be cool and dense enough to permit both neutral gas (Zickgraf et al. 1989, Kraus et al. 2007) and dust (Kastner et al. 2006) to exist.

While this model is successful in explaining the observations, there is currently no consensus as to either the detailed geometry of the circumstellar environment or the physical mechanism by which it could form. With bolometric luminosities ranging from $\sim 10^4 - 10^6 L_{\odot}$ implying initial masses ranging from $10 M_{\odot}$ to $\geq 60 M_{\odot}$ (Zickgraf et al. 1986, Gummertsbach et al.

1995, Maeder & Meynet 2001), there is no guarantee that the B[e] phenomenon is attributable to a single physical mechanism, since stars at the extremes of this distribution will follow very different post-main sequence evolutionary paths. Indeed, the inclusion of sgB[e] stars in such schemes is highly uncertain at present (Aret et al. 2012).

Despite their co-location in the Hertzsprung-Russell (HR) diagram (cf. Clark et al. 2005b, Aret et al. 2012), it is currently unknown whether sgB[e] stars and luminous blue variables (LBVs) may be physically identified with one another. As their name suggests, LBVs are massive evolved stars that are subject to pulsational instabilities that drive dramatic photometric and spectroscopic variability (e.g. Humphreys & Davidson 1994; Sect. 4.1) leading to changes in stellar radius, temperature and in some cases, mass loss rate and bolometric luminosity (e.g. Groh et al. 2009, Clark et al. 2009b and refs. therein). Conversely, sgB[e] stars have been considered to demonstrate little photometric variability (e.g. Zickgraf et al. 1986), with only a handful of known counter-examples (Sect. 4.1). Similarly, spectroscopic variability consistent with the canonical LBV ‘outbursts’ amongst sgB[e] stars has yet to be observed, although both classes of objects may show considerable overlap in spectral morphologies (e.g. Morris et al. 1996).

★ This work is partly based on observations collected at the European Southern Observatory (programme ID ESO 088.D-0352(A)).

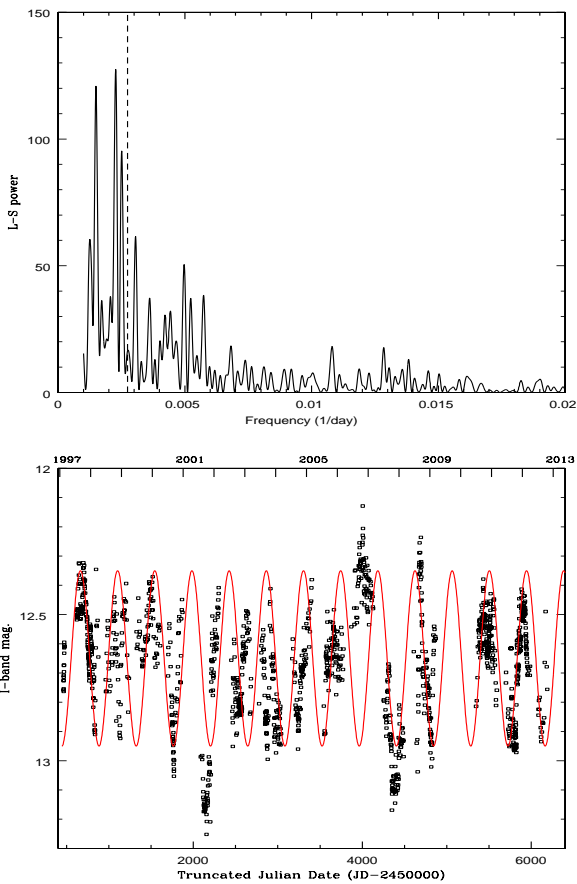


Fig. 2. Upper panel: un-detrended Lomb-Scargle periodogram for the I-band photometric data, with the position of 1/year indicated by the dashed line. No periodic signal is returned. Lower panel: lightcurve with a sine curve corresponding to the ~ 440 d period implied by the largest peak in the periodogram overplotted - the periodicity is not stable throughout the 16 year duration of observations.

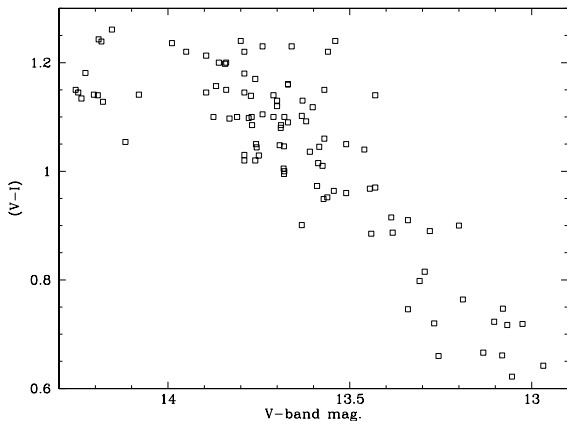


Fig. 4. Colour magnitude plot for S18.

In order to address these issues we present new observations of the sgB[e] LHA 115-S 18 (henceforth S18) which has been advanced as an LBV by a number of authors (e.g. Morris et al. 1996, van Genderen & Sterken 2002).

Since its discovery by Henize (1956), numerous observations have been made of S18. The optical spectrum of the star is characterised by strong emission in the Balmer series and

prominent He I lines (e.g. 6678Å and 7065Å) as well as a wealth of forbidden and permitted low excitation metallic lines (Fe II, [Fe II], Ti II, Cr II and O I). Following the behaviour observed in other sgB[e] stars, the high excitation lines are broader than the metallic lines. Moreover, they exhibit pronounced variability in profile and strength - the Balmer lines evolve from (asymmetric) single peaked to P Cygni profiles with absorption extending to 750kms^{-1} and vary in strength by a factor of ~ 3 (Zickgraf et al. 1989, Nota et al. 1996; see Table A.1 for a historical summary of optical spectroscopic studies). Recently, high resolution observations by Torres et al. (2012) revealed that the metallic lines are also variable, while Nota et al. (1996) reported changes in the radial velocities of these lines. However the most dramatic variability is seen in the He II 4686Å line, which has been observed to transition from absence to being comparable in strength to H β (Table A.1), with such changes occurring over short timescales (of the order of months; Shore et al. 1987).

Contrary to the conclusions of Shore et al. (1987) and Zickgraf et al. (1989), van Genderen & Sterken (2002) found S18 to be photometrically variable at optical wavelengths between 1987-1991. Modulation occurred on timescales from days to years, with peak-to-peak amplitudes ranging from $\sim 0.1 - 1.0$ mag (see Sect. 2.1.2. for a full description).

At other wavelengths, five International Ultraviolet Explorer UV observations between 1981 July to 1983 March were reported in Shore et al. (1987). No photometric variability above ~ 0.25 mag. was found but a number of high excitation wind features (He II, C IV, N V) were significantly variable. Two epochs of I band spectroscopy made by Shore et al. (1987; obtained on 1983 October 10) and Aret et al. (2012; obtained on 2005 December 10-11) share the same bulk morphology; being dominated by the Paschen series, Ca II 8491, 8542 and 8662Å and O I 8446Å. Conversely, K band spectroscopy presented by McGregor et al. (1989; obtained between 1987-89) and Morris et al. (1996; obtained in 1995 November) reveal evolution over this period, with the development of He I 2.058 μm and 2.112 μm and CO bandhead emission between the two epochs. At longer wavelengths, mid-IR spectroscopy and photometry provided by Kastner et al. (2010) and Bonanos et al. (2010) show that S18 supports a substantial IR-excess.

Finally a single epoch of Chandra X-ray observations made between 2002 May-October (source 6_20 of Antoniou et al. 2009) provides a weak detection of S18. While the count rate was too low to model the spectrum, they estimate a flux of $\sim 3 \times 10^{33}\text{erg s}^{-1}$ from this observation. Bartlett et al. (in prep.) present the results of an X-ray survey of sgB[e] stars within the Magellanic Clouds and provide a confirmatory XMM-Newton detection from an observation on 2003 December 18. Further details on data reduction and analysis are contained therein, but utilising the count rate of the EPIC-pn detector and Webpimms¹ it was possible to obtain a preliminary luminosity estimate of $\sim 3.9 \pm 0.7 \times 10^{33}\text{erg s}^{-1}$.

The remainder of the paper is structured as follows: we present our new photometric and spectroscopic observations, data reduction and analysis in Sects. 2 and 3. In Sects. 4 and 5 we discuss the nature of S18 in light of these results and possible physical associations between sgB[e] stars, massive binaries and LBVs. Finally we summarise our findings in Sect. 6.

¹ Assuming $n_H = 6 \times 10^{20}\text{ cm}^{-2}$ (corresponding to the column density in the direction of the SMC; Dickey & Lockman 1990), $\Gamma = 1.7$ (similar to that adopted by the 2XMM survey; Watson et al. 2009) and a distance of $\sim 61 \pm 3\text{ kpc}$ (Hilditch et al. 2005).

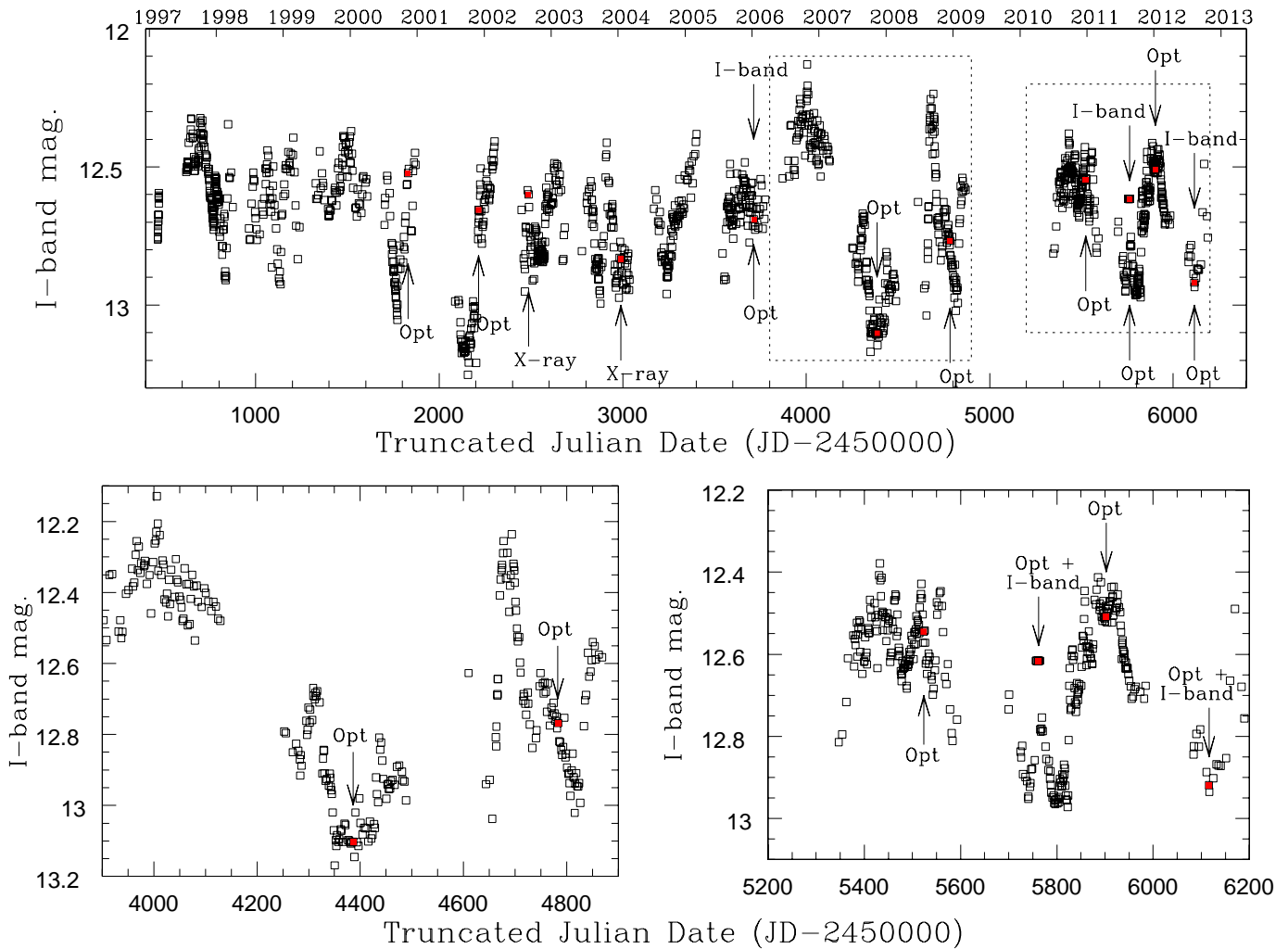


Fig. 1. Top panel: plot of the 1997-2012 OGLE-II, -III and -IV lightcurve data for LHA 115-S 18 with the timings of optical blue- (Massey & Duffy 2001, Torres et al. 2012 and this work) and far-red (Aret et al. 2012 and this work) spectroscopic and X-ray (Antoniou et al. 2009, Bartlett et al. in prep.) observations indicated. The nearest photometric data points to each observation are given by the filled red symbols. Note that the spectrum of Massey & Duffy and the first epoch of Torres et al. were obtained quasi-simultaneously and the date indicated for the first X-ray observation is the midpoint of the period over which observations were made. Photometric errors are smaller than the symbol size plotted. Lower panels: expanded presentation of two sub-sections of the lightcurve (indicated by dotted lines in the upper panel).

2. Data Reduction

2.1. Photometry

We utilized the Optical Gravitational Lensing Experiment data (OGLE-II, -III and -IV, Udalski et al. 1997, Udalski 2003) to investigate the long-term behaviour of S18 (OGLE-II designation: SMC_SC6 311169). OGLE has been regularly monitoring this object since 1997 with the 1.3-m Warsaw telescope at Las Campanas Observatory, Chile, equipped with three generations of CCD camera: a single $2k \times 2k$ chip operated in driftscan mode (OGLE-II), an eight chip 64 Mpixel mosaic (OGLE-III) and finally a 32-chip 256 Mpixel mosaic (OGLE-IV). Observations were collected in the standard V- and I-bands with the vast majority of images taken through the I-band filter.

OGLE I-band observations of S18 required an individually tailored approach to data reduction. During the period of OGLE-II observations the stellar brightness was well within the photometric range of the OGLE-II camera and measurements were derived with the standard OGLE DIA photometric reduction,

based on the image difference technique (Szymański 2005). However, during the OGLE-III and OGLE-IV phases the brightness of S18 on the survey frames turned out to be close to the saturation level of the CCDs. In particular this happened during observations with very good seeing conditions and as a result a few central pixels of the star saturated.

Therefore in the case of OGLE-III observations we decided to employ point spread function (PSF) photometry obtained with the DoPhot photometry program (Schechter et al. 1993; also provided by the OGLE-III photometry pipeline). The PSF approach is well suited to the treatment of saturated pixels at the cost of somewhat larger photometric errors. In the case of OGLE-IV images we manually derived S18 photometry, limiting ourselves to the images taken during seeing conditions where the object was not saturated. The photometric technique was identical to the OGLE standard photometric pipeline (Udalski 2003).

V-band images collected at all OGLE phases were reduced with the standard OGLE DIA technique. S18 was far from the saturation level in all OGLE V-band frames.

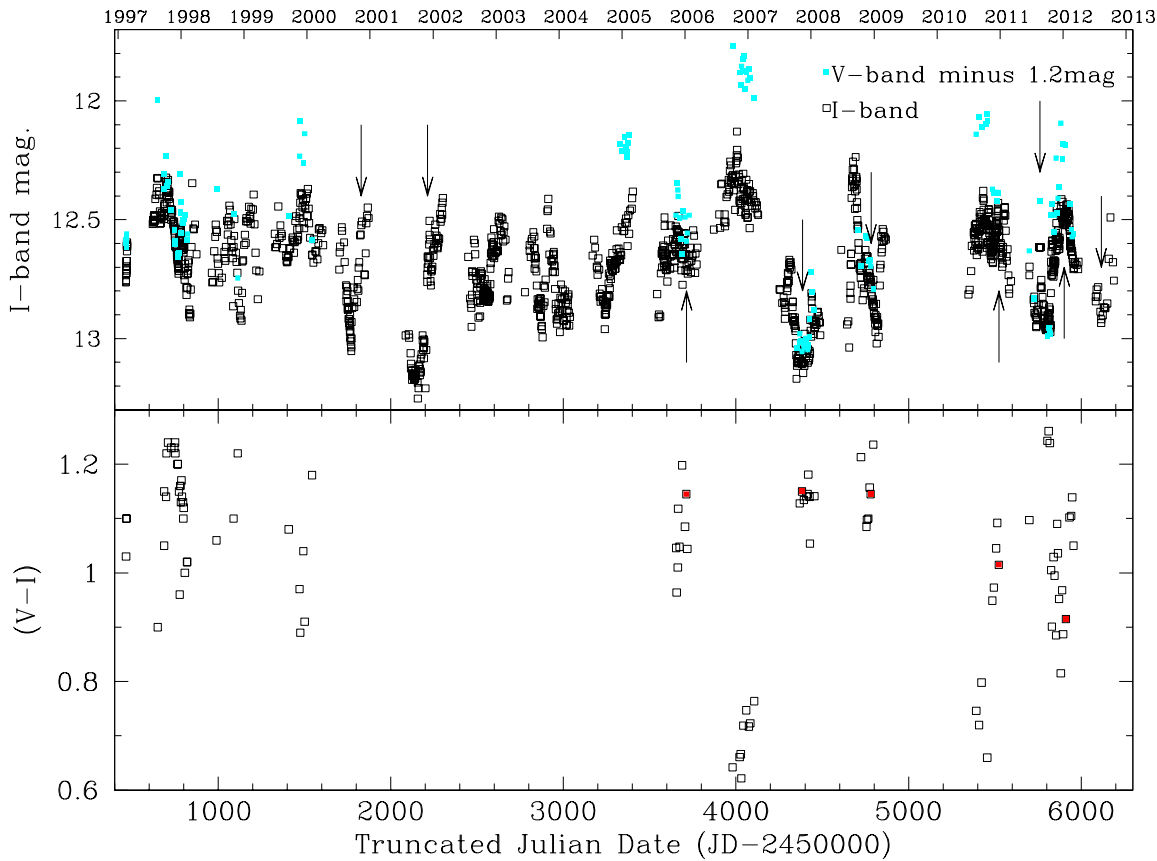


Fig. 3. Plots of V- and I-band OGLE lightcurves (with the V-band displaced by 1.2 mag. to enable easy comparison) and (V-I) colour index of time. Timings of optical spectroscopic observations indicated by arrows and (V-I) data within 9 d of an observation indicated by the red symbols (with the first four data points within 3 d).

All OGLE datasets were then combined after applying second order corrections for slightly different filter passbands. The complete dataset comprises 1365 I-band, 133 V-band and 100 (V-I) colour index measurements over the 16 year period from 1997-2012. Given the rapid variability present in the lightcurve we required both V- and I-band measurements on the same night to derive the (V-I) colour index. Errors on the OGLE DIA photometry (I-band: OGLE-II and OGLE-IV, V-band) are well below 10 mmag, while those for PSF photometry (I-band: OGLE-III) below 20 mmag. Given the much better sampled I-band lightcurve we base our discussion on this, utilising the V-band data to provide additional colour information.

2.2. Spectroscopy

The spectroscopic data presented in this work come from a number of sources. Firstly, we reproduce the full spectrum from Graus et al. (2012). This was obtained on 2010 November 24 with the MIKE echelle spectrograph on the Magellan Clay telescope and has a resolution of $\sim 28,000$ over the 3250\AA - 5050\AA wavelength range, with details on reduction provided in Graus et al. (2012).

Observations taken on 2011 July 20th and 21st and 2012 July 7th were made with the fibre-fed dual-beam AAOmega spectrograph on the 3.9 m Anglo-Australian Telescope (AAT) at the Australian Astronomical Observatory. The instrument was operated with the Two Degree Field ("2dF") multi-object system

as front-end. Light is collected through an optical fibre with a projected diameter of $2''.1$ on the sky and fed into the two arms via a dichroic beam-splitter with crossover at 5700\AA . Each arm of the AAOmega system is equipped with a $2k \times 4k$ E2V CCD detector and an AAO2 CCD controller. The blue arm CCD is thinned for improved blue response. The red arm CCD is a low-fringing type. On both occasions, the red arm was equipped with the 1700D grating, blazed at 10000\AA . This grating provides a resolving power $R = 10000$ over slightly more than 400\AA . In the 2011 run, the central wavelength was set at 8600\AA . In 2012, it was centred on 8690\AA . The exact wavelength range observed depends on the position of the target in the 2dF field.

During the 2011 run, the blue arm was equipped with the 1500V grating, which provides $R = 3700$ over $\sim 750\text{\AA}$. The central wavelength chosen was 4400\AA . During the 2012 run, we used grating 580V, giving $R = 1300$ over $\sim 2100\text{\AA}$. The central wavelength was set at 4800\AA .

Data reduction was performed using the standard automatic reduction pipeline *2dfr* as provided by the AAT at the time. Wavelength calibration was achieved with the observation of arc lamp spectra immediately before each target field. The lamps provide a complex spectrum of He+CuAr+FeAr+ThAr+CuNe. The arc line lists were revised and only those lines actually detected were given as input for *2dfr*. This resulted in very good wavelength solutions, with rms always < 0.1 pixels.

Sky subtraction was carried out by means of a mean sky spectrum, obtained by averaging the spectra of 30 fibres located

at known blank locations. With this procedure, any existing nebular emission is not removed.

The optical data from 2011 Decemeber 8 were taken with the ESO Faint Object Spectrograph (EFOSC2) mounted at the Nasmyth B focus of the 3.6m New Technology Telescope (NTT), La Silla. The EFOSC2 detector (CCD#40) is a Loral/Lesser, Thinned, AR coated, UV flooded, MPP chip with 2048×2048 pixels corresponding to 4.1'×4.1' on the sky. The instrument was in longslit mode with a slit width of 1.5'' using Grism 14 - resulting in a wavelength range of $\lambda\lambda 3095 - 5085 \text{ \AA}$ - and a grating of 600 lines mm^{-1} and a dispersion of 1 \AA pixel^{-1} yielding a wavelength range of $\lambda\lambda 6000 - 7150 \text{ \AA}$. The resulting spectra have a spectral resolution of $\sim 10 \text{ \AA}$. The data were reduced using the standard packages available in the Image Reduction and Analysis Facility (IRAF). Wavelength calibration was implemented using comparison spectra of Helium and Argon lamps taken through out the observing run with the same instrument configuration.

3. Data presentation and interpretation

3.1. Photometry

Photometrically, S18 is clearly highly variable on multiple timescales (Fig. 1), mirroring the findings of van Genderen & Sterken (2002) and raising the possibility that such behaviour has continued uninterrupted throughout the ~ 22 year period following their 1987-1991 observations. Given this, we followed the technique outlined in Bird et al. (2012) to search for periodic modulations in the I-band lightcurve. Briefly, we used the fast implementation of the Lomb-Scargle periodogram (Press & Rybicki 1989) to search for periodicities between 2 d (the Nyquist frequency for daily sampled lightcurves) and 10^3 d (above which the finite length of the lightcurve compromised sensitivity). Given the difficulties in detecting high-frequency signals in the presence of low-frequency modulations we also attempted to de-trend the data. Moving in one day steps, a rolling-mean was calculated over a $\sim 50 - 300$ d time window to determine a detrending model which was then subtracted from the light curve.

No periodicity was identified (Fig 2). Despite the appearance of various subsets of the lightcurve (e.g. JDs $\sim 2455200 - 6100$) no quasi-period present is stable over the 16 year duration of the observations and hence we are forced to procede via a more qualitative analysis. van Genderen & Sterken (2002) identified 3 types of variability: (i) short-term variability on the timescale of days and $\sim 0.1 - 0.2$ mag amplitude, (ii) ~ 150 d modulation with amplitude $\sim 0.25 - 1.0$ mag. and (iii) a long term (~ 2 year) trend with amplitude ~ 0.7 mag upon which the other behaviour is superimposed. We find no evidence for the latter behaviour in our data, seeing no long-term trends in brightness, but can recognise the other variability described.

Specifically, we find S18 to vary between $I \sim 12.1 - 13.3$ mag over the course of our observations but cannot identify any prolonged 'quiescent' maxima or minima in this period. Rapid, low amplitude (~ 0.2 mag) modulation on timescales of days-weeks is present - e.g. the periods between JD $\sim 2453500-800$, 2453900-4150 and 2455250-5600 (Fig. 1). This may be superimposed on the larger amplitude fluctuations that correspond to the second variability type of van Genderen & Sterken (2002) - e.g. JD $\sim 2452100-300$ and 2454700-800. The latter events span a range of timescales and amplitudes and appear exemplified by the behaviour of S18 between JD $\sim 2454000-4800$ (Fig. 1). The initial fade of ~ 1 mag amplitude - upon which is superimposed

a short-lived ~ 0.2 mag flare - occurs over a period of 400 d and is followed by a ~ 0.85 mag brightening event of only ~ 50 d duration. Note that we *do not* claim that the two types of photometric variability are the result of physically distinct processes within the system and merely employ them as a qualitative description of the lightcurve; indeed it is entirely possible they may both be manifestations of the same underlying instability.

Interpretation of colour variability is likewise difficult and is complicated by the comparatively sparse and uneven sampling of the V-band data. van Genderen & Sterken (2002) report that at the photometric maxima corresponding to ~ 150 d variations the system appears bluer and we find such a broad description to be applicable to our data; the magnitude of variability appears larger in the V- rather than the I-band (Fig. 3). However this behaviour appears not to be simply proportional to the brightness of the system as is clear from the colour magnitude plot (Fig. 4); such a relationship is only apparent for $V \lesssim 13.6 - 13.8$ mag and below this variability occurs at constant colour. Indeed, the 'blue-ing' of the system appears to be associated with episodes of brightening, with the subsequent decay branch of the lightcurve occuring at redder colours ((V-I) ~ 1.2) - e.g. the 'flaring' episodes between JD $\sim 2450600-800$ and 2455700-6000. Unfortunately, better sampled data will be required to fully explore these relationships.

3.2. Spectroscopy

Globally, the four new blue-end spectra obtained between 2010 November and 2012 July fit seamlessly into the long-term pattern observed for S18 (Table A.1 and refs. therein), although the high resolution and signal to noise (S/N) ratio of three of the spectra enable us to identify qualitatively new behaviour. All four epochs are dominated by Balmer series emission lines, which demonstrated P Cygni profiles in all transitions in 2010 November and H γ and higher lines in 2011 December (Figs. 5-7)². Strong He II 4686 \AA emission was present in two spectra (2011 and 2012 July), weakly in emission in a third (2011 December) and completely absent in our highest S/N and resolution spectrum (2010 November). We highlight that the presence of strong He II 4686 \AA emission appears anti-correlated with P-Cygni profiles in the Balmer series in these data, with the 2011 December spectrum apparently representing a transitional case. Similar behaviour is visible in the spectra from 2001 and 2005-2008 (Torres et al. 2012), and also appears present in earlier observations (Table A.1).

The appearance of He II also heralds an increase in the strength of the higher Balmer series lines (Fig. 6) and we are also able to identify a corresponding increase in strength of weaker He I and He II lines which had hitherto been lost in the forest of low excitation metallic lines. Of particular interest are the appearance of N III 4634 \AA and 4640 \AA emission lines that also accompany He II 4686 \AA (Fig. 5). Conversely, while the wealth of low excitation metallic lines³ identified by previous studies are present in all four spectra, we find little indication of variability in their strength (cf. comparison of the 2010 November and 2011 July spectra; Fig. 5). Likewise, they demonstrate no appreciable evolution in width (FWHM $\sim 45 \pm 5 \text{ km s}^{-1}$; measured from the 2010 November spectrum) since the observations of Zickgraf et

² Velocities of $\sim 500 \pm 10 \text{ km s}^{-1}$ for the blue edge of the absorption component in H β and H γ were found for the 2010 November spectrum, but were not measurable for the 2011 December spectrum due to its lower S/N and resolution.

³ Ca I, Cr II, Fe I, Fe II, [Fe II], [S II], Si II, Ti II and V II.

al. (1989) and imply much slower outflow velocities than the Balmer and He I P Cygni profiles do. Unfortunately, comparison of the line widths of the low excitation species between epochs is not instructive due to the lower resolution of our remaining spectra, but we see no appreciable differences in radial velocity in our data.

We therefore arrive at a simple picture where the behaviour of high- and low excitation lines appears largely de-coupled, with the former showing dramatic variations in line profile and strength over timescales as short as months, while the latter remain largely unaffected. Moreover, this pattern appears qualitatively consistent with observations made over the past half century (Sect. 1.1 and Table A.1).

The observations available in the 6000-7200Å and 8400-8900Å windows likewise indicate that the overall spectral morphologies remain largely unchanged from previous epochs (Sect. 1.1; Figs. 7 & 8). Specifically, and as expected, H α and the Paschen series and a number of He I lines are strongly in emission, although the I-band spectrum is dominated by emission from Ca II and O I. Other low excitation species present and in emission are Fe II, Si II and N I. Forbidden [O I] 6300Å line is also in emission; while consistent with a [N II] identification we suspect the inflection in the blue flank of H α is instead due to the run of absorption in the stellar wind (also seen in other sgB[e] stars such as R126; Zickgraf et al. 1986). Finally we identify TiO bandhead emission, as has previously been observed (Zickgraf et al. 1989).

Unfortunately, the low excitation emission lines (e.g. [O I], [O II], Ca II and [Ca II]) employed by Kraus et al. (2010) and Aret et al. (2012) to determine disc kinematics are either absent, outside our coverage, or observed at too low a resolution to impart information on the velocity structure of the emitting region. However, in the absence of the shell-type emission line profiles that arise from obscuration of the stellar disc by an intervening circumstellar disc (cf. S65; Kraus et al. 2010) we infer the system is not observed edge-on.

3.3. Photometric/spectroscopic comparison

We may utilise our well sampled optical lightcurve to place the spectroscopic observations into context (Figs. 1 & 3); noting that unfortunately the latter sample a restricted photometric range ($I \sim 13.10 - 12.51$ mag), albeit including local maxima and minima⁴. Nevertheless, the data suggest that the changes in spectral morphology - and in particular the appearance of He II 4686Å emission - is *not* uniquely correlated with photometric magnitude (Table A.1). This apparent lack of correlation is exemplified by the spectra obtained in 2010 November and 2011 July, where the strength of the high excitation emission features in the spectra differ greatly (Figs. 5 and 6) but for which the I-band magnitudes are identical to within ~ 0.07 mag. At the times of the two observations the extended photometric behaviour of the star was rather different, respectively exhibiting rapid low amplitude variability and at the peak of an rapid (~ 60 d) ~ 0.35 mag ‘flare’ (Fig. 1), which might be supposed to be a cause of the different spectral morphologies. However, He II 4686Å emission is present in both the 2011 and 2012 July spectra - obtained in local photometric minima and maxima - implying a lack of a clear correspondence between lightcurve behaviour and spectral morpholo-

⁴ van Genderen & Sterken (2002) report that the spectrum presented by Zickgraf et al. (1989) - in which He II 4686Å was absent - was obtained during a photometric maximum with $V \sim 13.3$; comparable in magnitude to the peak in our lightcurve around JD ~ 2455000 .

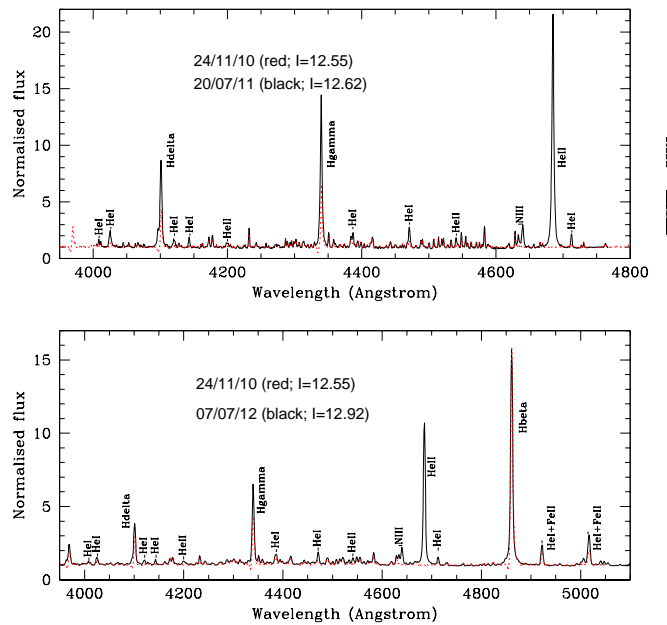


Fig. 6. As Fig. 5 but spectra scaled to compare the stronger emission features.

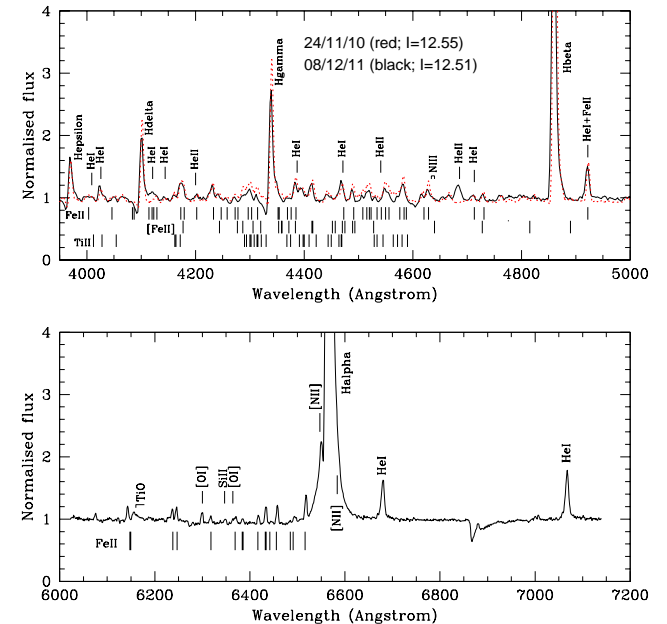


Fig. 7. As Fig. 5 but with the low resolution spectrum from 2011 December 8 - the only epoch for which coverage extends to H α and the He I 6678 and 7065Å transitions. Note the peak intensity of H α is $\sim 35\times$ continuum at this time.

gies. Nevertheless, our limited dataset is consistent with the possibility that while He II 4686Å emission may occur in any photometric state, a lack of emission is only associated with brighter states. Unfortunately, with only 5 quasi-contemporaneous observations (Fig. 3) we are unable to draw any conclusions regarding correlations to the (V-I) colour; again, more frequent spectroscopic sampling will be required to explore any such behaviour.

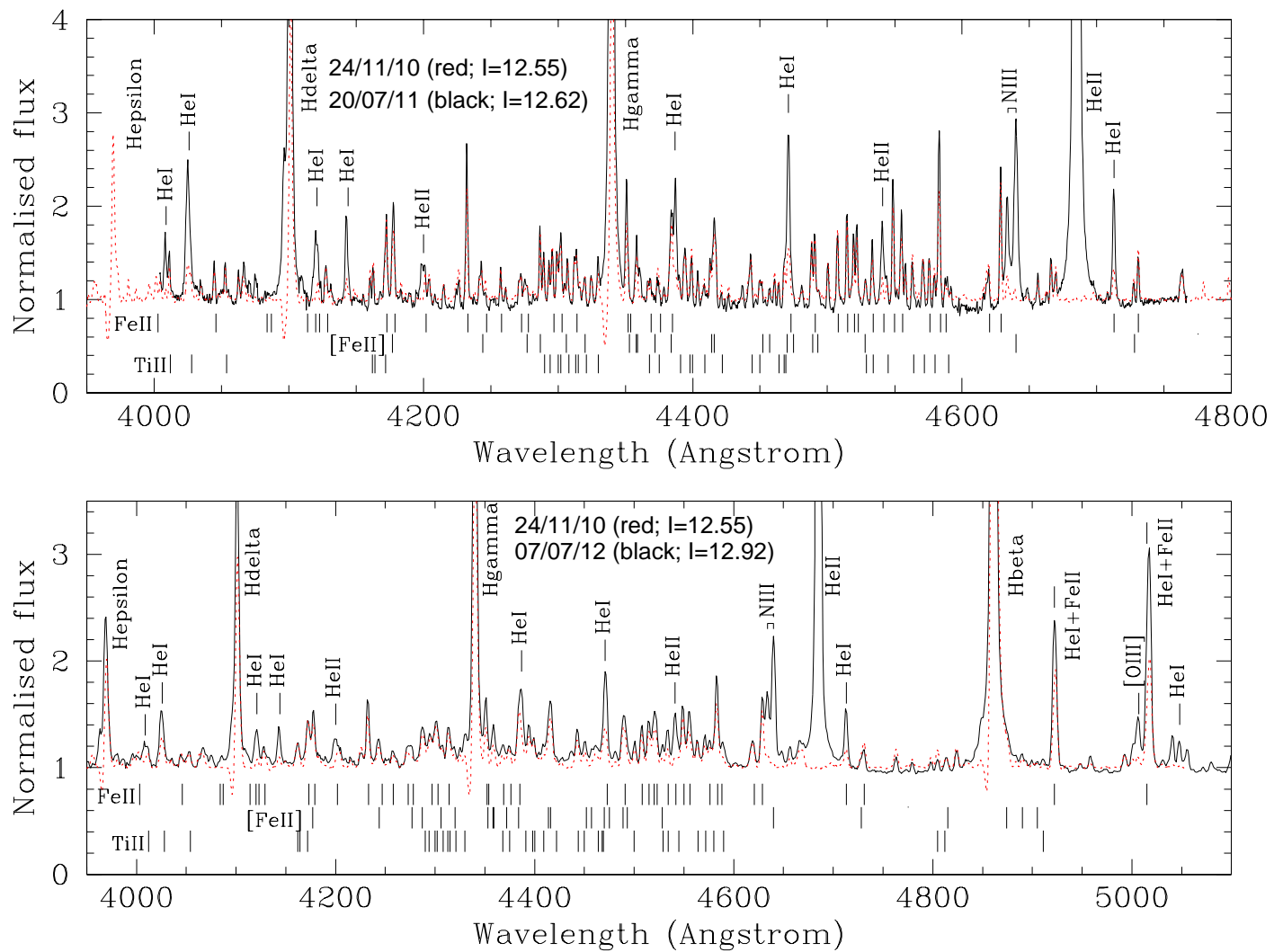


Fig. 5. Comparison of blue-end optical spectra obtained in 2010 November, 2011 July and 2012 July, after the resolution of the former has been degraded to match that of the latter two spectra (which themselves differ in resolution and wavelength coverage; Sect. 2). Prominent transitions are indicated as are the I-band magnitudes on the dates of the observations. Following the line identifications of Zickgraf et al. (1989), additional weak emission lines from low excitation metallic species such as Ca I, Cr II, Fe I, [S II], Si II and V II are not shown for reasons of clarity.

4. The circumstellar environment of S18

So how is S18 to be understood in the context of other sgB[e] stars? A defining property of such stars is the presence of a cool equatorial disc or torus, comprising neutral and molecular gas and warm dust. The presence of e.g. Ca II emission (Fig. 8) implies cool, dense conditions ($\sim 5000\text{K}$, $\sim 10^9\text{ cm}^{-3}$; Hamann & Simon 1988) which are shielded from the ionising flux of the central star. Likewise O I 8446Å requires a dense transitional zone between H I and H II regions ($10^9 - 10^{10}\text{ cm}^{-3}$; Grandi 1980) for Ly β pumping to drive it strongly into emission (cf. Wd1-9; Clark et al. 2013a) and the discovery of Raman-scattering lines also requires neutral hydrogen to be present (Torres et al. 2012). The presence of TiO and CO bandhead emission (Sect. 1.1 and Fig. 7) likewise points to the presence of cool, dense molecular gas (Morris et al. 1996, Liermann et al. 2010). At longer wavelengths the mid-IR properties of S18 suggest the presence of warm ($\sim 800\text{K}$) dust with a probable crystalline silicate composi-

tion; both properties consistent with other sgB[e] stars (Kastner et al. 2006, 2010, Bonanos et al. 2010).

In these regards S18 appears to conform to the stereotype of a sgB[e] star (Zickgraf et al. 1985), where the low excitation spectrum is formed within - or in the case of the Ly α and β pumped lines such as O I 8446Å and Fe II 8490Å - on the surface layer of a cool dense torus surrounding the central star. The optical-IR continuum excess demonstrated by S18 (Zickgraf et al. 1989) would then result from a combination of thermal bremsstrahlung from the stellar wind and/or disc and thermal emission from the warm dust which also resides in the torus (e.g. Porter 2003).

Recent spectroscopic observations suggest that the neutral gaseous component in sgB[e] stars is detached from the central star (e.g. Kraus et al. 2010, Liermann et al. 2010 & Aret et al. 2012). Kastner et al. (2006, 2010) arrived at a similar conclusion from analysis of the mid-IR properties of sgB[e] stars and, by analogy to lower mass AGB stars, postulated that the dust resides in long lived quasi-Keplerian disc surrounding a binary system which formed from mass lost in a previous common-

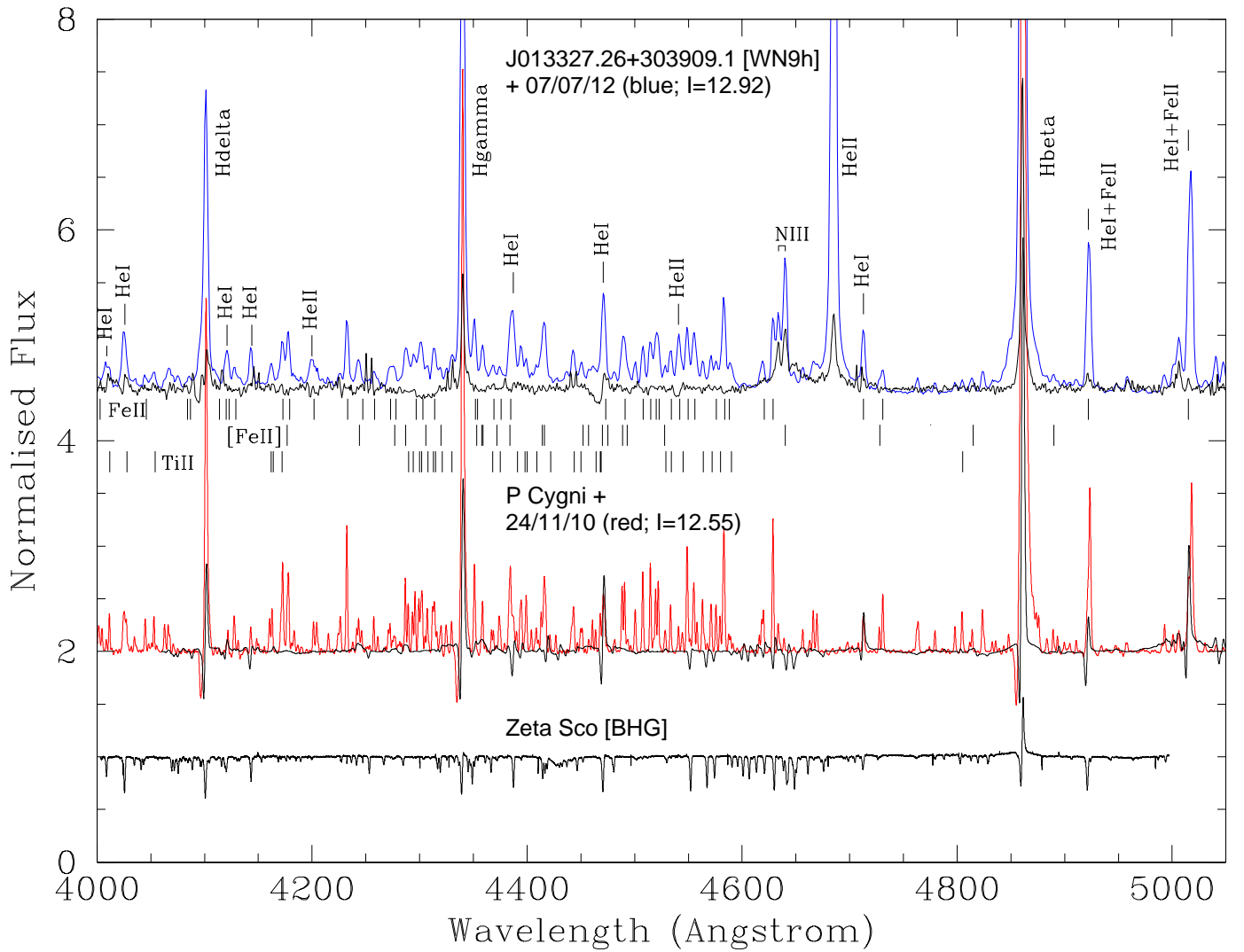


Fig. 9. Comparison of 2010 ('cool' state) and 2012 ('hot' state) spectra versus the B1 Ia+ hypergiant ζ^1 Sco, P Cygni and the M33 WN9h star J013327.26+303909.1 with major transitions indicated. Note that in the absence of a cool toroid circumstellar envelope, we would not expect the three comparison spectra to demonstrate the rich low-excitation metallic emission spectrum of S18.

envelope/mass transfer phase. Support for this geometry has been provided by interferometric observations of the galactic B[e] stars CI Cam and MWC300 (Thureau et al. 2009, Wang et al. 2012) and the sgA[e] star HD 62623 (Meilland et al. 2010), which imply ring-like geometries for the circumstellar material.

While our spectroscopic observations lack the wavelength coverage and resolution to address the kinematics of the disc/torus, the spectra of S18 presented by Aret et al. (2012) reveal that the higher excitation [Ca II] lines are broader than the lower excitation [O I] lines, as anticipated for Keplerian rotation.

Consequently, it is possible to see why the low-excitation component of the spectrum of S18 is, in terms of variability, essentially decoupled from the high-excitation component, if the former arises in a largely static, quasi-Keplerian, viscous, detached disc while the latter is associated with an intrinsically variable star. Following the analysis of classical Be star discs by Okazaki et al. (1991) we may obtain an estimate of the viscous timescale of such a disc. We make the simplifying assumption that the gaseous component of the quasi-Keplerian disc is isothermal and adopt a representative disc temperature

of $T_d \sim 6000\text{K}^5$ and adopt representative inner disc radii of $R_d \sim R_*$ (i.e. it extends to the stellar surface at R_*) and $R_d \sim 10R_*$ (motivated by the apparent truncation of the disc in LHA 115-S 65; Kraus et al. 2010, Aret et al. 2012).

Under these conditions the viscous timescale in the disc, t_{vis} , is given by $(\alpha \times (H/r)^2 \times \Omega_{K(r)})^{-1}$, where H is the disk scale-height and $\Omega_{K(r)}$ is the Keplerian angular frequency at radius r . Adopting $M_* \sim 19M_\odot$ and $R_* \sim 33R_\odot$ (e.g. Aret et al. 2012) for $r = R_*$ we have $\Omega_K \sim 0.8$ d and $H/r \sim c_s/(r \times \Omega_K) \sim 0.02$ and $\Omega_K \sim 25$ d and $H/r \sim 0.06$ for $r = 10R_*$ (where c_s is the sound speed). From these values we find $t_{\text{vis}} \sim 20/(\alpha/0.3)$ yr and $\sim 62/(\alpha/0.3)$ yr respectively (where α is the viscosity parameter and t_{vis} is proportional to the inverse of the disc temperature). Therefore the combination of the relatively low temperature (in contrast to classical Be star discs) and large inner radius adopted results in a long viscous timescale and hence timescale

⁵ The mid-point Kraus et al. (2010) derive from the strength of [O I] emission lines, noting that as with classical Be stars the assumption of an isothermal disc is likely violated in practice.

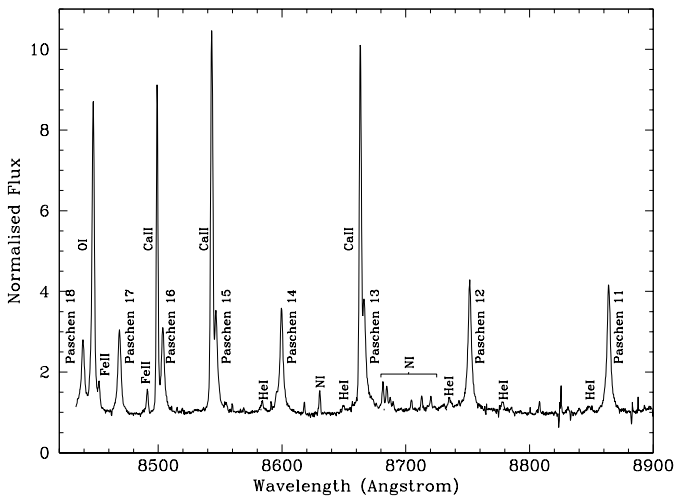


Fig. 8. I-band spectrum of S18 from 2011 July 20 with major transitions indicated.

of variability in response to changes in the bulk properties of the disc/torus.

Despite this, both Nota et al. (1996) and Torres et al. (2012) report line profile variability in the Fe II lines - one might expect rapid changes in the disc properties in response to changes in the ionising flux or, by analogy to classical Be stars, due to the impulsive injection of matter (Rivinius et al. 1998).

5. The nature of the central star(s)

What is the nature of the hot, luminous central star in S18? No uncontaminated photospheric features are present in any published spectra so we are forced to infer stellar properties from the highly variable high-excitation emission-line spectrum. Following the suggestions of Zickgraf et al. (1989) and Nota et al. (1996), in Fig. 9 we plot exemplar spectra from November 2010 (henceforth the ‘cool’ spectrum/phase) and July 2012 (the ‘hot’ spectrum/phase) against representative spectra of the early blue hypergiant (BHG) ζ^1 Sco, the BHG/LBV P Cygni and a sample WN9h star, J013327.26+303909.1. As described by these authors, in both cool and hot states S18 shows gross similarities to the latter two objects. Specifically, (i) a simple spectrum comprising narrow Balmer and He I emission lines in the cool phase, with the former showing P Cygni profiles and (ii) the disappearance of P Cygni line profiles and the development/strengthening of He I, He II and N III emission in the hot phase; all characteristic features of the spectra of P Cygni-type LBVs and WN9h stars, respectively (e.g. Najarro 2001, Crowther & Smith 1997). Neither the hot nor the cool spectrum resembles that of the early BHG ζ^1 Sco and, by extension, field blue supergiants, because such stars do not support winds of sufficiently high mass loss rate to drive the Balmer series into the intense emission present in S18 (Table 1 and Clark et al. 2012b and refs. therein).

Under the assumption that the high-excitation emission line spectrum arises in a stellar wind, the blue edge of the P Cygni profiles in the Balmer series provides a lower limit to the wind velocity in the cool phase ($\sim 500 - 750 \text{ km s}^{-1}$). Such a value is broadly consistent with expectations for early-mid B supergiants (BSG)/BHG, but much faster than expected for LBVs such as P Cygni (Table 1 and Clark et al. 2012b). Conversely the mass loss rate ($\sim 3 \times 10^{-5} M_{\odot} \text{ yr}^{-1}$; Zickgraf et al. 1989, derived from

line profile modeling of the Balmer series) is much higher than expected for BSGs and BHGs but consistent with known LBVs (Clark et al. 2012b)⁶. The disappearance of P Cygni profiles in the WN9h spectrum is explicable in terms of the full ionisation of the stellar wind due to an increase in stellar temperature, although one might also expect such behaviour to be accompanied by changes in the stellar wind; note, for example, the greater wind velocity of WN9h stars with respect to P Cygni-type LBVs (for similar mass loss rates; Table 1). Under such a picture the spectrum obtained in 2011 December, which demonstrates weak He II emission and P Cygni profiles in the higher Balmer transitions, would represent an intermediate state.

An obvious interpretation of these spectroscopic data is that S18 transitions directly between P Cygni-type LBV and WN9h spectral types. However there are several *caveats* to such an hypothesis. Firstly, Zickgraf et al. (1989) presented a simple model atmosphere fit to the UV-IR spectral energy distribution of S18 and, assuming a temperature of $\sim 25000 \text{ K}$, a bolometric correction of -2.5 mag and a distance to the SMC of 60 kpc , inferred a luminosity of $\log(L/L_{\odot}) \sim 5.6$ in the cool phase. The lower bolometric correction derived for P Cygni suggests a downwards revision to $\log(L/L_{\odot}) \sim 5.3$; significantly lower than in the comparison stars listed in Table 1 (although low luminosity examples are known - e.g. Clark et al. 2009a).

Secondly, in both cool and hot phases the emission line spectrum is unprecedentedly strong with respect to P Cygni-type LBVs and WN9h stars; this being particularly noteworthy for He II 4686 \AA (Fig. 9; Nota et al. 1996). Moreover, He II 4686 \AA was seen to be double peaked at one epoch, with the blue peak of greater intensity (with corresponding asymmetric profiles in the Balmer series and He I; Nota et al. 1996). Such asymmetries are observed in other B[e] stars (e.g. Zickgraf 2003) and are also common in classical Be stars (Okazaki 1991); in all cases heralding a departure from spherical symmetry for the circumstellar environment, as we infer for S18. This is in contrast to the spherical geometry typically assumed for the winds of P Cygni-type LBVs and WN9h stars (although Nota et al. (1996) report similar asymmetries for a subset of the Ofpe/WN9 stars they studied). Another unexpected spectral peculiarity in S18 is the absence of P Cygni profiles in the He I emission lines in the cool spectrum when clearly present in the Balmer series.

Finally, the X-ray detection ($L_X \sim 3 \times 10^{33} \text{ erg s}^{-1}$; Antoniou et al. 2009, Bartlett et al. in prep.) strongly suggests a binary nature for S18. The canonical X-ray luminosity for a single massive star ($L_X \sim 10^{-7} L_{\text{bol}}$; Berghoefter et al. 1997) implies $L_X \sim 1.6 \times 10^{32} \text{ erg s}^{-1}$ for S18; over an order of magnitude lower than observed (Sect. 1.1) and hence requiring an additional source of X-rays to be present within the system. Therefore in addition to a contribution from the circumstellar disc/torus one might also suppose additional spectroscopic contamination from a binary companion; we return to this below.

5.1. S18 as a LBV

With these caveats in mind, the simplest explanation for the spectroscopic and photometric properties of S18 remains that it hosts an LBV. Indeed, a physical link between sgB[e] stars and

⁶ Nevertheless, this pattern of wind properties is observed in the unusual BHG Wd1-5; a star which is thought to be the result of binary driven mass loss and that is also thought to approach the Eddington limit (Clark et al. 2013b).

Table 1. Stellar parameters of comparison stars in Fig. 9

Star	$\log(L/L_{\odot})$	T_{eff} (kK)	\dot{M} ($10^{-6}M_{\odot}\text{yr}^{-1}$)	v_{∞} (km s^{-1})	BC (mag)	Ref.
ζ^1 Sco (B1 Ia ⁺)	5.93	17.2	1.55	390	-1.6	1
P Cygni (B1 Ia ⁺ /LBV)	5.85	19.0	30.0	185	-1.8	2
Mean WN9h	5.7	27.6	18.5	450	-2.9	3

Tabulation of the bolometric luminosity (L), effective temperature (T_{eff}), mass loss rate (\dot{M}), terminal wind velocity (v_{∞}) and bolometric correction (BC) for the comparison spectra in Fig. 9. References are ¹Clark et al. (2012b), ²Najarro (2001) and ³Crowther & Smith (1997); the value for the final entry is the mean of the modeling results for the four WN9h stars analysed by the latter authors. The broadly comparable luminosities reveal that the changes in spectral morphology are primarily the result of changes in temperature and wind parameters.

LBVs has been proposed on the basis of photometric variability in a number of stars⁷.

S18 appears to reside in a region of the H-R diagram prone to pulsational instabilities (e.g. Cantiello et al. 2009, Saio 2011) and clearly shows the presence of the rapid microvariability present in many LBVs and luminous super-/hypergiants (the α -Cygni variables; van Leeuwen et al. 1998)⁸ but the rapid, high-amplitude variability it demonstrates appears at variance with typical canonical LBV excursions (e.g. Spoon et al. 1994)⁹. Nevertheless such rapid variability is not completely unknown, being present in a handful of local LBVs and also the extragalactic SNe imposters, presaging both giant eruptions (η Carinae, HD5980 and SN 1954J; Frew 2004, Smith & Frew 2011, Breysacher 1997 and Tammann & Sandage 1968) and *bona fide* SNe (SN 2010mc and possibly SN2009ip; Ofek et al. 2013 and Sect. 6), although in the case of SN2000ch a decade of such behaviour has yet to lead to either outcome (Pastorello et al. 2010). S18 may be identified with SN2000ch in this regard, although the amplitude of variability is significantly lower, most closely resembling SN 1954J in the 4 years leading up to its eponymous outburst (Tammann & Sandage 1968; see also SN2009ip (Sect.6)).

The colour behaviour of S18 also differs from that of LBV excursions; leading to the system becoming bluer in the rising branches of the lightcurve and showing much greater variance in comparison to canonical examples (cf. Fig. B.1, derived from data presented by Spoon et al. 1994). The colour behaviour of normal LBVs - which become redder as they brighten - arises from the simultaneous expansion (contraction) and cooling (warming) of the photosphere as the star transits

⁷ The binary RMC 4 (Zickgraf et al. 1996), LHA 120-S 22 (Shore et al. 1990,1992; van Genderen & Sterken 1999; Sterken 2011) LHA 120-S 134 (Stahl et al. 1984, van Genderen vanG01) and J013459.47+303424.7 (Clark et al. 2012a) are all reported as photometrically variable at UV-optical wavelengths, albeit from considerably sparser datasets than considered here.

⁸ Following the analysis of the blue supergiant HD 50064 by Aerts et al. (2010), an identification of these variations with strange mode oscillations would appear an interesting hypothesis, especially given the long-term changes in both amplitude and timescale of this behaviour. However, the likely progenitor mass of S18 ($\sim 20 - 25M_{\odot}$ via comparison to the isochrones of Groh et al. 2013) is lower than that expected for stars encountering this instability ($\sim 40M_{\odot}$; Aerts et al. 2010).

⁹ These consist of (i) microvariations, occurring over weeks to months and of low amplitude ($\lesssim 0.2$ mag), (ii) LBV excursion, occurring over years to decades and typically of $\sim 0.5 - 2.0$ mag amplitude and which are typically associated with colour changes in the sense that the star becomes redder as it brightens and (iii) giant eruptions, in which the star brightens by ≥ 2.0 mag over timescales ranging from days to years and in which the bolometric luminosity is not conserved (e.g. Humphreys & Davidson 1994, Lamers et al. 1998).

from WN10-11h to cool supergiant in ‘outburst’ and back again (e.g. AG Car; Groh et al. 2009, Groh priv. comm. 2012) and clearly cannot explain the behaviour observed here. Indeed the spectral evolution of S18 occurs over a temperature range for which the change in (V-I) colour index would be minimal (cf. Clark et al. 2005b).

We highlight that not all LBVs show this behaviour - for instance the SNe imposter SN 2000ch shows no colour/magnitude correlations during its rapid high amplitude flares (Fig. B.1; Pastorello et al. 2010). An additional complication with interpreting the behaviour of S18 is that the presence of a substantial circumstellar envelope - and a probable binary companion - may also contribute to the photometric variability; indeed the modeling of Zickgraf et al. (1989) suggests a continuum excess extending to optical wavelengths.

We may advance two different scenarios to explain the photometric variability, noting that they are not mutually exclusive. Firstly, the episodes in which S18 rapidly brightens and becomes bluer may be due to an increased contribution from the hot central star relative to the cool circumstellar disc/torus (and/or stellar wind) in the combined emergent spectrum. The lack of colour changes associated with ‘quiescent’ and fading branches of the lightcurve is more difficult to understand, but may represent quasi-simultaneous variability in both emission components. Moreover, we are unable to advance a physical mechanism for such stellar ‘pulsations’, although this is true for LBVs in general; for instance the pulsations Aerts et al. (2010) attribute to strange mode oscillations in HD 50064 are of substantially lower magnitude (~ 0.2 mag) to those observed here.

Alternatively the variability may be due to changeable circumstellar extinction, with comparable behaviour seen in both classical Be (de Wit et al. 2006) and Herbig Be stars (Lamers et al 1999). In classical Be stars this is observed for edge-on systems, where the gaseous disc projected against the star reduces continuum emission at short wavelengths, but contributes continuum emission at predominantly longer wavelengths from the portion of the disc *not* projected against the star, such that the system becomes fainter and redder as the disc optical depth increases. A variant of this scenario is assumed for Herbig Be stars, where variable stellar extinction is attributable to a clumpy, dusty circumstellar envelope.

However, a significant problem with such an hypothesis is the location of the obscuring material and the rapidity of changes. A comparison of the line profiles of S18 to e.g. those of the sgB[e] star LHA 115-S 65 suggest it is not seen edge-on (Zickgraf et al 1989, Kraus et al. 2010); therefore it appears unlikely that the circumstellar disc/torus could be responsible as is assumed for both classical and Herbig Be stars. Likewise, while the stellar winds of LBVs are known to be clumpy (Davies et al.

2005), such clumps are not expected to be sufficiently dense to provide the requisite obscuration of the stellar disc.

Irrespective of the physical mechanism, a key observational finding of this research is that there is no clear correlation between photometric and spectroscopic variability; for example the hot and cool phase spectral states in 2010 November and 2011 July differed by only ~ 0.07 mag. Naively applying the respective bolometric corrections implied by the spectral morphologies (Table 1) would imply that the luminosity of S18 had increased by ≥ 0.44 dex over this period; however such a conclusion is tempered by the potentially highly variable continuum contribution from the stellar wind/circumstellar envelope at these wavelengths. Bearing this important *caveat* in mind, changes in bolometric luminosity are not unprecedented in *bona fide* LBVs, having been observed in e.g. AFGL 2298 and Romano’s star (Clark et al. 2009b, Maryeva & Abolmasov 2012). Moreover, while S18 has not been observed to transition to the cool hypergiant phase that characterises many LBV excursions, the range of spectroscopic variability it exhibits (WN9h \leftrightarrow P Cygni-type LBV) mirrors the behaviour of Romano’s Star (Maryeva & Abolmasov 2012).

Finally, we note that the mid-IR properties of S18 appear to exclude the presence of the cool dust that characterises the circumstellar ejecta of many LBVs (Clark et al. 2003, Bonanos et al. 2010).

5.2. S18 as a binary system

The presence of highly variable He II 4686Å emission in the spectrum of S18 has long been attributed to binarity (Shore et al. 1987, Zickgraf et al. 1989). Furthermore Nazé et al. (2012) find that in the absence of a binary companion LBVs are intrinsically X-ray faint, strongly suggesting that our X-ray detection of S18 indicates the presence of an unseen binary companion (Sects 1.1 and 4.0). Two options therefore present themselves; accretion onto a compact object or wind collision leading to shocked material in a massive binary.

Several examples of X-ray binaries with sgB[e]-like mass donors are known. SS433 has a complex, dusty circumstellar environment (Clark et al. 2007) and demonstrates highly variable He II 4686Å emission (Fabrika & Bychkova 1990), but is several orders of magnitude brighter at X-rays than S18 (Cherepaschuk et al. 2005). CI Cam and IGR J16318-4848 appear to provide better comparisons; while distances to both stars are uncertain, at the lower end of the ranges quoted in the literature their quiescent fluxes are comparable to that of S18 (Bartlett et al. 2012, Barragán et al. 2009).

Spectroscopically, CI Cam also bears a close resemblance, even to the extent of He II 4686Å emission being present in quiescence (e.g. Clark et al. 1999, Hynes et al. 2002). Nevertheless, the long term photometric and spectroscopic behaviours of CI Cam and S18 are very different, with the former much less variable and demonstrating consistently weaker He II 4686Å emission (Clark et al. 2000, Hynes et al. 2002). Indeed, He II 4686Å only approached the strength observed in S18 when CI Cam exhibited an X-ray flare in 1998 April. The outburst was replicated at optical wavelengths, where CI Cam brightened by over 2.5 magnitudes (Clark 2000); to date no such behaviour has been observed for S18.

Conversely, there are a number of observational precedents that suggest that S18 could comprise a massive interacting binary system. Firstly, both GG Carina and VFTS698 are spectroscopically confirmed sgB[e] binaries with apparent circumbi-

nary discs/toroids (Gosset et al. 1985, Kraus et al. 2013, Dunstall et al. 2012), while Kastner et al. (2006, 2010) suggest such a configuration from their modeling of the mid-IR excess of sgB[e] stars. Secondly, the X-ray luminosity of S18 is well within the range observed for colliding wind systems ($\sim 10^{32} - 10^{35}$ ergs $^{-1}$; Gagne et al. 2012) and is comparable to that of the sgB[e] star Wd1-9; a massive compact interacting binary within the starburst cluster Wd1 (Clark et al. 2008, 2013a).

Finally, variable He II 4686Å emission is a key observational signature of a number of massive binary systems, where it is the result of an additional contribution to the ionising flux from shocks arising in a wind-wind collision zone. Under such a scenario we might explain the increase in strength of the He II 4686Å line *in tandem* with the apparent transition to a hot, WN9h phase as a result of the increase in wind velocity expected for a star of such a spectral type (Table 1), which in turn would lead to a stronger wind collision shock.

In this regard three LBVs are of interest. η Carina is an eccentric, long period ($P_{\text{orb}} \sim 5.52$ yr), colliding wind binary that shows orbital modulation in the He II 4686Å line (Steiner & Daminelli 2004; Teodoro et al. 2012) - albeit much weaker than seen in S18 - and strong X-ray emission (maximum $L_X \sim 1.3 \times 10^{35}$ erg s $^{-1}$; Ishibashi et al. 1999).

The second, HD 5980, is a close, eccentric, eclipsing binary ($P_{\text{orb}} \sim 19.26$ d; Sterken & Breysacher 1997) comprising an LBV primary (WN3 \leftrightarrow WN11h/B1.5 Ia $^+$; Niemela 1988, Koenigsberger et al. 1994, Drissen et al. 2001, Heyardi-Melayari et al. 1997) and a WN4 secondary (Breysacher et al. 1982) with a possible third O4-6 component in a wide orbit (Foellmi et al. 2008). Highly variable He II 4686Å emission has been observed both before and after its 1993-5 outbursts (e.g. Moffat et al. 1998, Breysacher & François 2000, Koenigsberger et al. 2010). This is likely the result of wind/wind collisional effects, although an intrinsic contribution from one or both stellar winds cannot be excluded. Unlike S18, this emission does not appear to be absent at any (orbital) phase. X-ray emission is present and of a comparable magnitude to S18 ($L_X \sim 1.7 \times 10^{34}$ erg s $^{-1}$; Nazé et al. 2002, 2007).

The final star is the SNe imposter SN 2000ch, which also demonstrates an asymmetric doubled lined He II 4686Å line in quiescence (Pastorello et al. 2010). These authors draw direct comparison between SN 2000ch, S18 and indeed HD 5980 on this basis, suggesting that all three could be binaries and we note that both SN 2000ch and HD 5980 also exhibit the rapid photometric variability seen in S18, albeit of much greater amplitude.

Therefore the multiwavelength properties of S18 are at least consistent with other luminous colliding wind binaries containing LBVs. Given the unprecedented strength and variability in the He II 4686Å line it would be of considerable interest to search for periodic variability indicative of orbital modulation, especially since the inclination of S18 (Zickgraf et al. 1989) disfavours identification of binary reflex motion and no evidence of eclipses or ellipsoidal modulation is present in the lightcurve. Moreover, higher S/N X-ray observations in order to distinguish between relativistic-accretor and colliding-wind scenarios would be of considerable interest.

6. Concluding remarks

Photometric and spectroscopic observations of S18 over the past half century demonstrate that it is a highly dynamic and complex system; at odds with the historic picture of sgB[e] stars as essentially static objects. The cool circumstellar disc/torus shows little

spectroscopic variability over the course of this period; appearing to be essentially decoupled from the central stellar source, which is delineated by the high excitation emission component of the composite spectrum and is highly variable.

Our observations reveal that, trivially, S18 satisfies the eponymous classification criteria of LBVs. However, this does not imply that the physical causes of its variability are the same as those of canonical S-Doradus type objects such as AG Car. Specifically, the (assumed) ‘stellar’ spectrum - and the speed of its evolution - is more extreme than canonical examples. Moreover, the photometric variability of S18 is difficult to interpret in the framework of known LBVs, although the rapidity of the ‘flaring’ does appear to mirror that of some ‘SNe imposters’. The colour behaviour is likewise atypical and, surprisingly, we see no apparent correlation between spectroscopic and photometric behaviours, raising the possibility that the bolometric luminosity of S18 varies over time.

The detection of X-ray emission adds to the weight of evidence that S18 hosts an unseen binary companion, with observations apparently favouring a colliding wind system over a relativistic accretor, although the latter cannot currently be excluded. In this respect the combination of a powerful wind at relatively modest luminosity inferred by Zickgraf et al. (1989) is of interest, since it mirrors the properties of the BHG Wd1-5, which is thought to have evolved through a phase of binary-driven mass-loss (Clark et al. submitted). Model atmosphere analysis of S18 to determine if it shares the anomalous chemistry of Wd1-5 would be welcome, but is currently premature given its aspherical circumstellar envelope and the possibility of spectral contamination resulting from binarity.

These observational properties highlight the importance of S18 for a number of reasons. Firstly it strengthens the physical link posited between sgB[e] stars and LBVs and also the possibility that the B[e] phenomenon is linked with binarity; specifically that the circumstellar/binary disc is the direct result of binary evolution (e.g. Zickgraf 2003, Kastner et al. 2010, Kraus et al 2013). The presence of a detached, quasi-Keplerian viscous disc/torus is attractive since the decadal viscous timescale of such a structure would naturally explain the relative lack of variability in its spectral signatures in comparison to the central star(s). Indeed, to the best of our knowledge, and in contrast to classical Be stars, disc-loss and/or reformation has not been observed in sgB[e] stars. This would be explicable if the viscous (and hence dissipation/formation) timescales of discs around sgB[e] stars is significantly longer than that of classical Be stars due to their greater physical extent and lower temperatures.

Recent observational studies suggest both a high binary fraction amongst massive stars and that the majority of these systems will in turn interact (Sana et al. 2012). Given this, the suggestion that sgB[e] stars may be currently undergoing, or have recently undertaken, significant binary-driven mass-loss/transfer is important, since it would allow for their identification with this brief evolutionary phase. Other examples of this phenomenon would then be the sgB[e] star Wd1-9 (Clark et al. 2013a) and RY Scuti (e.g. Smith et al. 2011); the latter system is of particular relevance since the authors speculate that the mass transfer in this system is mediated by episodic, LBV-like events.

Finally, the presence of a massive detached disc/torus associated with an apparent LBV raises issues regarding the nature of its demise, given recent observational and theoretical predictions that such stars can serve as the immediate progenitors of core-collapse SNe (e.g. Gal-Yam & Leonard 2009, Groh et al. 2013). Indeed the latter authors find this occurs for stars in

the range $\log(L_{\text{bol}}/L_{\odot}) \sim 5.3 - 5.6$ ($M_{\text{initial}} \sim 20 - 25M_{\odot}$); directly spanning the luminosity range we infer for S18 (Sects. 5 and 5.1). Following from this it is immediately tempting to draw parallels between S18 and the B3 Ia progenitor of SN1987A (Walborn et al. 1989), which was of similarly modest luminosity ($\log(L_{\text{bol}}/L_{\odot}) \sim 5.1 \pm 0.1$), must have been associated with a circumstellar disc and for which a binary interaction/merger scenario has been proposed that would have left the progenitor resembling a sgB[e] star in its immediate aftermath (e.g. Morris & Podsiadlowski 2009).

Another intriguing comparator is SN2009ip. Initially classified as a SNe-imposter, between 2009-11 it demonstrated rapid photometric variability of a similar, but more extreme nature than S18 (Sect. 5.1; Smith et al. 2010, Foley et al. 2011, Pastorello et al. 2012). During this period, its spectrum was also not dissimilar to that of S18 in gross terms, being dominated by Balmer series He I and Fe II line emission in the blue and Paschen series, Ca II and O I emission in the red, although outflow velocities were substantially greater than implied for S18 and a greater mass ($\sim 50 - 80M_{\odot}$) also inferred. In 2012 it displayed two eruptions; the nature of the first event is uncertain, with core-collapse SNe, pair-production instability and binary merger all being proposed, while the second is assumed to result from the interaction of rapidly expanding ejecta with existing circumstellar material (Mauerhan et al. 2013, Pastorello et al. 2012, Prieto et al. 2012, Soker & Kashi 2013). Both Smith et al. (2013) and Levesque et al. (2012) conclude that dust was present in the circumstellar material, with the latter authors suggesting a disc-like geometry and a possible origin in binary-driven mass-loss (although an origin in the recent photometric outbursts is also viable). As such, the possibility that S18 represents a lower mass analogue of this highly unusual energetic transient is particularly exciting.

Acknowledgements. We thank the anonymous referee for their insightful comments which have greatly improved this manuscript. This research is partially supported by the Spanish Ministerio de Ciencia e Innovación (MICINN) under grant AYA2010-21697-C05-01/05. The OGLE project has received funding from the European Research Council under the European Community’s Seventh Framework Programme (FP7/2007-2013) / ERC grant agreement no. 246678 to AU. The AAT observations have been supported by the OPTICON project (observing proposals 2011A/014 and 2012A/015), which is funded by the European Commission under the Seventh Framework Programme (FP7). Drs Carlos González-Fernández and Amparo Marco prepared and executed some of the AAT observations. Finally, we wish to thank Paco Najarro, Atsuo Okazaki and Jose Groh for their valuable input.

References

- Aerts, C., Lefever, K., Baglin, A., et al. 2010, *A&A*, 513, L11
Aret, A., Kraus, M., Muratore, M. F. & Borges Fernandes, M. 2012, *MNRAS*, 423, 284
Antoniou, V., Zezas, A., Hatzidimitriou, D. & McDowell, J. C. 2009, *ApJ*, 697, 1695
Azzopardi, M., Vigneau, J. & Macquet, M. 1975, *A&AS*, 22, 285
Azzopardi, M. & Breysacher, J., 1979, *A&A*, 75, 120
Azzopardi, M., Breysacher, J., Muratorio, G. 1981, *A&A*, 95, 191
Barragán, L., Wilms, J., Pottschmidt, K., et al. 2009, *A&A*, 508, 1275
Barba, R. H., Niemela, V. S., Baume, G. & Vazquez, R. A. 1995, *ApJ*, 446, L23
Bartlett, E. S., Clark, J. S., Coe, M. J. et al. 2013, *MNRAS*, 429, 1213
Berghoefter, T. W., Schmitt, J. H. M. M., Danner, R., Cassinelli, J. P. 1997, *A&A*, 322, 167
Bird, A. J., Coe, M. J., McBride, V. A. & Udalski, A. 2012, *MNRAS*, 423, 3663
Bonanos, A. Z., Lennon D. J., Köhlinger, F., et al. 2010, *AJ*, 140, 416
Breysacher, J., Moffat, A. F. J. & Niemela, V. 1982, *ApJ*, 257, 116
Breysacher, J. 1997, *Luminous Blue Variables: Massive stars in transition*. ASP Conference Series, Vol. 120, ed. A. Nota and H. Lamers, p. 227
Breysacher, J. & François, P. 2000, *A&A*, 361, 231
Cantiello, M., Langer, N., Brott, I. et al. 2009, *A&A*, 499, 279
Cherepashchuk, A. M., Sunyaev, R. A., Fabrika, S. N., et al. 2005, *A&A*, 437, 561

- Clark, J. S., Steele, I. A., Fender, R. P. & Coe, M. J. 1999, *A&A*, 348, 888
- Clark, J. S., Miroshnichenko, A. S., Larionov, V. M., et al. 2000, *A&A*, 356, 50
- Clark, J. S., Egan, M. P., Crowther, P. A., et al. 2003, *A&A*, 412, 185
- Clark, J. S., Negueruela, I., Crowther, P. A. & Goodwin, S. P. 2005, *A&A*, 434, 949
- Clark, J. S., Larionov, V. M. & Arkharov, A. 2005b, *A&A*, 435, 239
- Clark, J. S., Barnes, A. D. & Charles, P. A. 2007, *MNRAS*, 380, 263
- Clark, J. S., Muno, M.P., Negueruela, I., et al., 2008, *A&A*, 347, 147
- Clark, J. S., Davies, B., Najarro, F. et al. 2009a, *A&A*, 504, 429
- Clark, J. S., Crowther, P. A., Larionov, V. M., et al. 2009b, *A&A*, 507, 1555
- Clark, J. S., Castro, N., Garcia, M., et al. 2012a, *A&A*, 541, A146
- Clark, J. S., Najarro, F., Negueruela, I. et al. 2012b, *A&A*, 541, A145
- Clark, J. S., Ritchie, B. W. & Negueruela, I. 2013a, *A&A*, submitted
- Clark, J. S., Ritchie, B. W., Najarro, F., Langer, N. & Negueruela, I. 2013, *Science*, submitted
- Crowther, P. A. & Smith, L. J. 1997, *A&A*, 320, 500
- Davies, B., Oudmaijer, R. D. & Vink, J. S. 2005, *A&A*, 439, 1107
- de Wit, W. J., Lamers, H. J. G. L. M., Marquette, J. B. & Beaulieu, J. P. 2006, *A&A*, 456, 1027
- Dickey, J. M. & Lockman, F. J. 1990, *ARA&A*, 28, 215
- Drissen, L., Crowther, P. A., Smith, L. J., et al. 2001, *ApJ*, 545, 484
- Dunstall, P. R., Fraser, M., Clark, J. S., et al. 2012, *A&A*, 542, 50
- Fabrika, S. N. & Bychkova, L. V. 1990, *A&A*, 240, L5
- Fitzgerald, M. P. 1970, *A&A*, 4, 234
- Foellmi, C., Koenigsberger, G., Georgiev, L., et al. 2008, *RMxAA*, 44, 3
- Foley, R. J., Berger, E., Fox, O. et al. 2011, *ApJ*, 732, 32
- Frew, D. J., 2004, *JAD*, 10, 6
- Gagne, M., Fehon, G., Savoy, M. et al. 2012, *arXiv1205.3510G*
- Gal-Yam, A. & Leonard, D. C. 2009, *Nature*, 458, 865
- Georgiev, L., Koenigsberger, G., Hillier, D. J., et al. 2011, *AJ*, 142, 191
- Gosset, E., Hutsemekers, D., Swings, J. P. & Surdej, J. 302, 409 1985, *A&A*,
- Grandi, S. A. 1980, *ApJ*, 238, 10
- Graus, A. S., Lamb, J. B. & Oey, M. S. 2012, *ApJ*, 759, 10
- Groh, J. H., Hillier, D. J., Daminieli, A., et al. 2009, *ApJ*, 698, 1698
- Groh, J. H., Meynet, G. & Ekström, S. 2013, *A&A*, 550, L7
- Gummersbach, C. A., Zickgraf, F.-J., Wolf, B., 1995, *A&A*, 302, 409
- Hamann, F. & Simon, M. 1988, *ApJ*, 327, 867
- Henize, K. G., 1956, *ApJS*, 2, 315
- Heydari-Malayeri, M., Rauw, G., Esslinger, O. & Beuzit, J.-L. 1997, *A&A*, 322, 554
- Hilditch, R. W., Howarth, I. D. & Harries, T. J. 2005, *MNRAS*, 357, 304
- Humphreys, R. M. & Davidson, K. 1994, *PASP*, 111, 1124
- Hynes, R. I., Clark, J. S., Barsukova, E. A., et al. 2002, *A&A*, 392, 991
- Ishibashi, K., Corcoran, M. F., Davidson, K. et al. 1999, *ApJ*, 524, 983
- Kastner, J. K., Buchanan, C., Sargent, B. A. & Forrest, W. J. 2006, *ApJ*, 638, L29
- Kastner, J. K., Buchanan, C., Sahai, R., Forrest, W. J. & Sargent, B. A. 2010, *AJ*, 139, 1993
- Koenigsberger, G., Moffat, A. F. J., St-Louis, N., et al. 1994, *ApJ*, 436, 301
- Koenigsberger, G., Guinan, E., Auer, L. & Georgiev, L. 1995, *ApJ*, 452, L107
- Koenigsberger, G., Georgiev, L., Hillier, D. J., et al. 2010, *AJ*, 139, 2600
- Kraus, M., Borges Fernandes, M. & de Araújo, F. X. 2007, *A&A*, 463, 627
- Kraus, M., Borges Fernandes, M. & de Araújo, F. X. 2010, *A&A*, 517 A30
- Kraus, M., Oksala, M., Nickeler, D. et al. 2013, *A&A*, 549, A28
- Lamers, H. J. G. L. M., Bastiaanse, M. V., Aerts, C. & Spoon, H. W. W. 1998, *A&A*, 335, 605
- Lamers, H. J. G. L. M., Beaulieu, J. P. & de Wit, W. J. 1999, *A&A*, 341, 827
- Levesque, E. M., Stringfellow, G. S., Ginsburg, A. G., Bally, J. & Keeney, B. A. 2012, *ApJ*, in press [arXiv1211.4577L]
- Liermann, A., Kraus, M., Schnurr, O. & Borges Fernandes, M. 2010, *MNRAS*, 408, L6
- Lindsay, E. M. 1955, *MNRAS*, 115 248
- Maeder, A. & Meynet, G. 2001, *A&A*, 373, 555
- Maryeva, O. & Abolmasov, P. 2012, *MNRAS*, 419, 1455
- Massey, P. & Duffy, A. S. 2001, *ApJ*, 550, 713
- Mauerhan, J. C., Smith, N., Silverman, J. M., et al. 2013, *MNRAS*, in press
- McGregor, P. J., Hyland, A. R. & McGinn, M. T., 1989, *A&A*, 223, 237
- Meilland, A. Kanaan, S., Borges Fernandes, M., et al. 2010, *A&A*, 512, A73
- Moffat, A. F. J., Marchenko, S. V., Bartzakos, P., et al. 1998, *ApJ*, 497, 896
- Morris, P. W., Eenens, P. R. J., Hanson, M. M., Conti, P. S. & Blum, R. D. 1996, *ApJ*, 470, 597
- Morris, T. & Podsiadlowski, Ph. 2009, *MNRAS*, 399, 515
- Najarro, F., 2001, *ASP Conf. Ser.* 233, *P Cygni 2000: 400 Years of Progress*, ed. M. de Groot & C. Sterken (San Francisco, CA:ASP), 133
- Nazé, Y., Hartwell, J. M., Stevens, I. R., et al. 2002, *ApJ*, 580, 225
- Nazé, Y., Corcoran, M. F., Koenigsberger, G. & Moffat, A. F. J., 2007, *ApJ*, 658, L25
- Nazé, Y., Rauw, G., Hutsemekers, D., 2012, *A&A*, 538, A47
- Niemela, V. S., 1988, in *ASP Conf. Ser. Col. 1, Progress and opportunities in southern hemisphere optical astronomy. The CTIO 25th anniversary symposium*, eds. V. M. Blanco & M. M. Phillips (San Francisco: ASP), 381
- Nota, A., Psaquali, A., Drissen, L. et al. 1996, *ApJS*, 102, 383
- Okazaki, A. T. 1991, *PASJ*, 43, 75
- Oksala, M. E., Kraus, M., Arias, L. et al. 2012, *MNRAS*, 426, L56
- Pastorello, A., Botticella, M. T., Trundle, C., et al. 2010, *MNRAS*, 408, 181
- Pastorello, A., Cappellario, E., Insera, C., et al. 2012, *ApJ*, submitted [arXiv:1210.3568]
- Press, W. H., Rybicki, G. B., 1989, *ApJ*, 338, 277
- Prieto, J. L., Brimacombe, J. Drake, A. J. & Howerton, S., 2012, *ApJL*, submitted [arXiv:1210.3347]
- Porter, J. M. 2003, *A&A*, 398, 631
- Rivinius, Th., Baade, D., Stefl, S. et al. 1998, *A&A*, 333, 125
- Saio, H. 2011, *MNRAS*, 412, 1814
- Sana, H., de Mink, S. E., de Koter, A. et al. 2012, *Science*, 337, 444
- Sanduleak, N., 1978, *IBVS*, 1389
- Schechter, P. L., Mateo, M., Saha, A. 1993, *PASP*, 105, 1342
- Shore, S. N. & Sanduleak, N. 1982 in *NASA. Goddard Space Flight Center Advances in Ultraviolet Astronomy* p602
- Shore, S. N., Sanduleak, N. & Allen, D. A. 1987, *A&A*, 176, 59
- Shore, S. N., 1990, *IAU Circular No.* 5005
- Shore, S. N., 1992, *ASP Conf. Ser.*, 22, 342
- Smith, N. & Frew, D. J. 2011, *MNRAS*, 415, 2009
- Smith, N., Miller, A., Li, W., et al. 2010, *AJ*, 139, 1451
- Smith, N., Gehrz R. D., Campbell, R. et al. 2011, *MNRAS*, 418, 1959
- Smith, N., Mauerhan, J. C., Kasliwal, M. M. & Burgasser, A. J. 2013, *MNRAS*, submitted [arXiv1303.0304]
- Soker, N. & Kashi, A. 2013, *ApJ*, 764, L6
- Spoon, H. W. W., de Koter, A., Sterken, C., Lamers, H. J. G. L. M. & Stahl, O. 1994, *A&AS*, 106, 141
- Stahl, O., Leitherer, C., Wolf, B. & Zickgraf, F.-J. 1984, 131, L5
- Stahl, O., Wolf, B., de Groot, M. J. H. & Leitherer, C., 1985, *A&AS*, 61, 237
- Stahl, O. 1986, *A&A*, 164, 321
- Stahl, O., Jankovics, I., Kovács, J., et al. 2001, *A&A*, 375, 54
- Steiner, J. E., Daminieli, A., 2004, *ApJ*, 612, L133
- Sterken, C. & Breysacher, J. 1997, *A&A*, 328, 269
- Sterken, C. 2011, *IBVS*, 6000, 1
- Szymański, M. K. 2005, *AcA*, 55, 43
- Tammann, G. A. & Sandage, A., 1968, *ApJ*, 151, 825
- Teodoro, M., Daminieli, Arias, J. I. et al. 2012, *ApJ*, 746, 73
- Thureau, N. D., Monnier, J. D., Traub, W. A., et al. 2009, *MNRAS*, 398, 1309
- Torres, A. F., Kraus, M., Cidale, L. S., et al. 2012, *MNRAS*, 427, L80
- Udalski, A., Kubiak, M. & Szymanski, M. 1997, *AcA*, 47, 319
- Udalski, A., 2003, *AcA*, 53, 291
- Ofek, E. O., Sullivan, M., Cenko, S. B., et al. 2013, *Nature*, 494, 65
- van Genderen, A. M. & Sterken, C., 1999, *A&A*, 349, 537
- van Genderen, A. M. 2001, *A&A*, 366, 508
- van Genderen, A. M. & Sterken, C., 2002, *A&A*, 386, 926
- van Leeuwen, F., van Genderen, A. M. & Zegelaar, I. 1998, *A&AS*, 128, 117
- Walborn, N. R., Prevot, M. L., Prevot, L. et al. 1989, *A&A*, 219, 229
- Wang, Y., Weigelt, G., Kreplin, A. et al. 2012, *A&A*, 545, L10
- Watson, M. G., Schröder, A. C., Fyfe, D. et al. 2009, *A&A*, 493, 339
- Zickgraf, F.-J., Wolf, B., Stahl, O., Leitherer C. & Klare, G., 1985, *A&A*, 143, 421
- Zickgraf, F.-J., Wolf, B., Stahl, O., Leitherer, C. & Appenzeller, I., 1986, *A&A*, 163, 119
- Zickgraf, F.-J., Wolf, B., Stahl, O. & Humphreys, R. M. 1989, *A&A*, 220, 206
- Zickgraf, F.-J., Kovas, J., Wolf, B. et al. 1996, *A&A*, 309, 505
- Zickgarf, F. J. 2003, *A&A*, 408, 257

Appendix A: Summary of historical and current data for S18

Appendix B: Colour magnitude behaviour of LBVs and SNe imposters

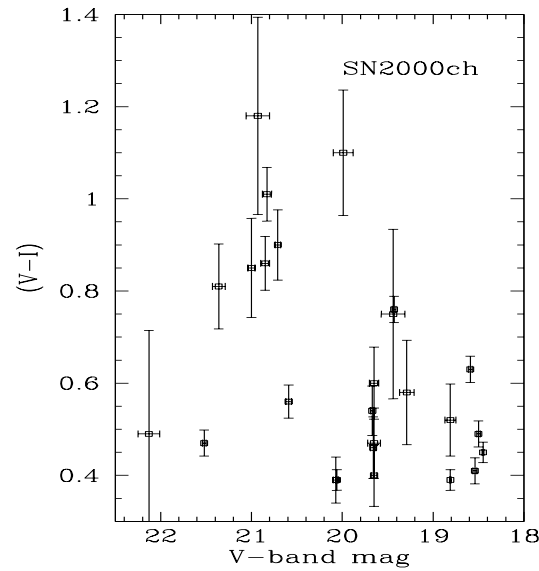
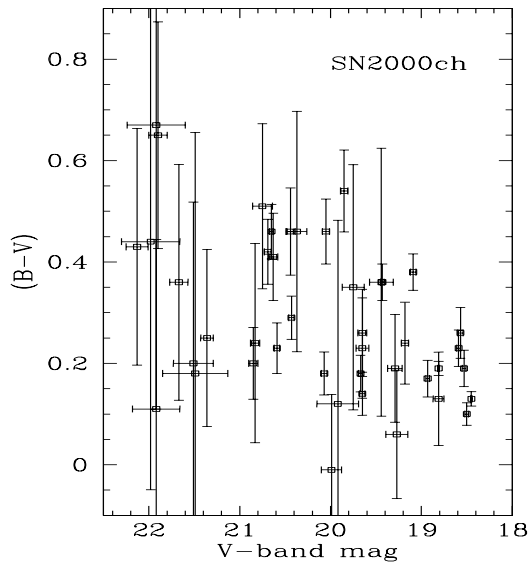
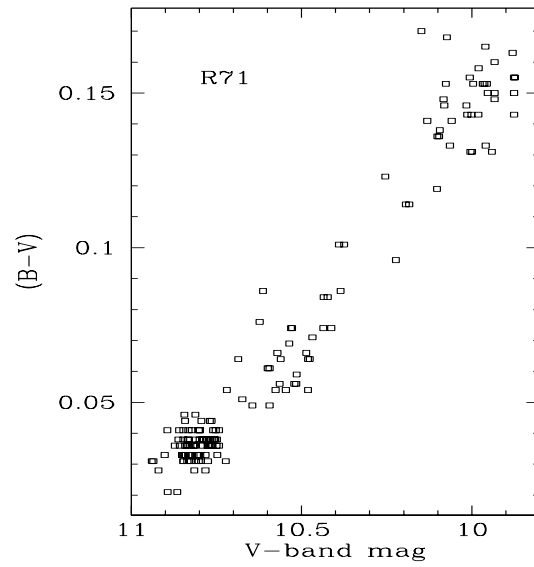
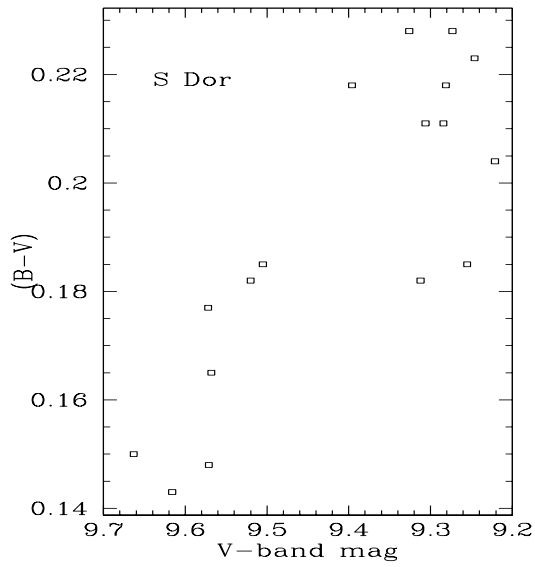
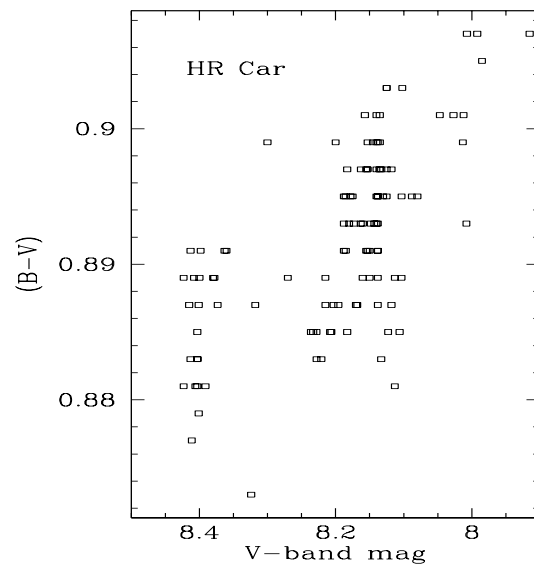
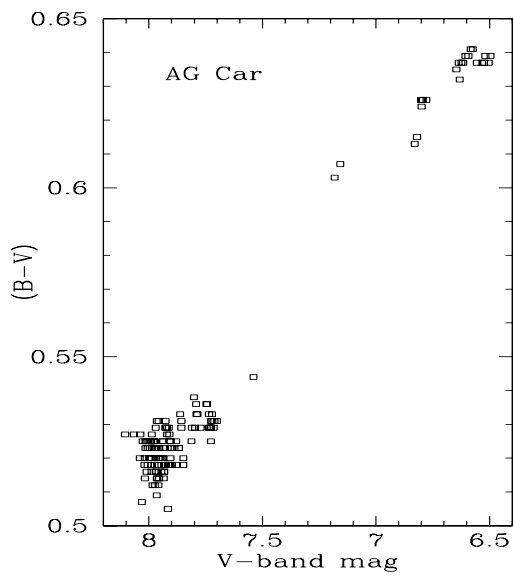


Fig. B.1. Colour magnitude plots of 4 known LBVs in the Galaxy and Magellanic clouds and of the SNe imposter SN2000ch (=NGC2403 LBV1).

Table A.1. Optical spectroscopic summary

Date	I-band	Comments	Reference
< 1955	-	H α , H β , H γ and He II 4686Å in emission	Lindsay (1955)
1967 July 14	-	Balmer emission to He I. He II 4686Å absent	Sanduleak (1978)
1972-74	-	H α , H β , H γ , He I in emission. No mention of He II 4686Å	Azzopardi et al. (1975)
1977 September 17	-	Balmer emission to He I. He II 4686Å emission comparable to H β	Sanduleak (1978)
1978 January 27	-	H β to H13 P Cygni emission. He II 4686Å and Fe II (multiplet 24) in emission	Azzopardi et al. (1981)
1978 July 16	-	H α to H11 and He II 4686Å in emission	Shore et al. (1987)
1981 July 13	-	Balmer series and He II 4686Å in emission	Shore & Sanduleak 1982
1982 March 22	-	Balmer series and He II 4686Å in emission He II 4686Å ~50% weaker than 1981 July 13	Shore & Sanduleak 1982
1983 Oct 10	-	H α to H11 and He II 4686Å in emission	Shore et al. (1987)
1983 December 17	-	H α to H11 and He II 4686Å in emission. P Cygni profile for higher Balmer lines but not H α or He II 4686Å	Shore et al. (1987)
1987 Nov. 7	-	H α to H δ and He I 5876Å in P Cygni emission. He II 4686Å absent	Zickgraf et al. (1989)
1991 September 17-20	-	H α to H δ and He I in emission. Double peaked He II 4686Å	Nota et al. (1996)
2000 October 11-14	12.52	H β to H δ in emission. He II 4686Å absent	Massey & Duffy (2001)
2000 October 13	12.52	H α , H β and He I 6678Å in P Cygni emission. He II 4686Å absent	Torres et al. (2012)
2001 November 24	12.66	H α , H β and He I 6678Å in emission. He II 4686Å absent	Torres et al. (2012)
2005 December 10	12.69	H α , H β , He I 6678Å and He II 4686Å in emission	Torres et al. (2012)
2007 October 3-4	13.10	H α , H β , He I 6678Å and He II 4686Å in emission	Torres et al. (2012)
2008 November 13	12.79	H α , H β , He I 6678Å and He II 4686Å in emission	Torres et al. (2012)
2010 November 24	12.55	H β to He I in P Cygni emission, He II 4686Å absent	This work
2011 July 11	12.62	H α to H δ , He I 6678Å and 7065Å and He II 4686Å in emission He II 4686Å stronger than H γ	This work
2011 December 8	12.51	H β to He I in emission, He II 4686Å weakly in emission H β single peaked, H γ to He I P Cygni profiles	This work
2012 July 07	12.92	H β to He I in (single peaked) emission, He II 4686Å stronger than H γ	This work

I-band magnitudes quoted are from OGLE-II,-III and -IV (Sect. 2.1). Note that emission lines are single peaked unless otherwise noted. Lindsay (1955), Sanduleak (1978), Azzopardi et al. (1975), Shore & Sanduleak (1982). Shore et al. (1987) and Torres et al. (2012) do not present all the spectra described in these works. Additionally Azzopardi & Breysacher (1975) detected He II 4686Å in emission in 1977 October via an objective prism survey.